Vol. 48 No. 1 Journal of the Communications Research Laboratory March 2001
Printed in Tokyo, Japan pp. 135–142

4.3 Millisecond Pulsar Timing Observations at CRL

By
Yuko HANADO, Yasuhisa SHIBUYA, Mizuhiko HOSOKAWA,
Mamoru SEKIDO, and Michito IMAE

ABSTRACT

Millisecond pulsars are attractive as future reference clocks, because of their highly stable pulse timing. Communications Research Laboratory (CRL) aims to apply millisecond pulsars to the construction of a new time scale, and have developed a millisecond pulsar observation system using the 34 m antenna at Kashima Space Research Center. Since the 34 m antenna is rather small for the receiving of weak signals from millisecond pulsars, we had to develop a highly sensitive observation system. This system is equipped with an acousto-optic spectrometer (AOS) for wide-band observations, and a special digital processor for performing numerous pulse integrations in real time. Using this system, we have started weekly observation of PSR1937+21 at the 34 m antenna in S-band since November 1997. The residuals of pulse phases for two years show some drift, and more precise timing analysis is required. Current observation precision is 2.9 μs for one day's observation, which shows that the 34 m antenna's performance is enough for the highly precise timing measurement of the weak pulse signals from millisecond pulsars.

Keywords: Time standard, Millisecond pulsar, AOS

1. Introduction

A pulsar is a celestial body that emits light and/or radio waves that seem to blink on and off at a precise regular frequency. Pulsars are actually thought to be neutron stars that are rotating at high speed. They emit beams of electromagnetic waves from their magnetic poles, which are shifted from their rotational axis, with the result that periodic pulses are observed in synchronization with their rotation. A pulsar with a pulse period (i.e., rotation period) of a few milliseconds is called a millisecond pulsar. The pulse periods of millisecond pulsars remain extremely stable for long periods. Figure 1 illustrates the frequency stability of two different millisecond pulsars[1]. As this figure shows, the frequency stability of PSR1855+09 is almost 10^{-15}, which rivals that of an atomic clock.

As a result of their high stability, it has been suggested that millisecond pulsars could form the basis of time scales and frequency standards. A time scale in which it is defined from the pulse period of a pulsar is called a pulsar time scale. Pulsar time scale has various unique advantages, such as a virtually indefinite life span and a complete lack of dependence on the Earth's motion and gravitational field. However, pulsars cannot be used as primary frequency standards because their inner workings are not yet entirely understood, and it is still difficult to construct an accurate model of all the phenomena that give rise to fluctuations. For reasons such as these, we are currently investigating methods for the construction of long-term stable systems incorporating atomic time scales, and we are trying to find practical applications for these methods[2][3][4]. We are also expecting our research to find applications in various other research fields. For example, the results can be used to compare different ephemerides[1] since they are reflected with high precision in the motion of the solar system. They can also be used to compare different coordinate systems[5] by comparing the positions determined with VLBI observations with the positions determined by timing observations. Millisecond pulsars can also be used as highly precise probes for detecting the minute effects of gravitational fields and interstellar matter in the propagation path. A detailed discussion of pulsar time scales can be found in reference[6].

Millisecond pulsar observations are also being made at many observatories overseas, including the 305 m antenna at Arecibo in Puerto Rico, the Nancay observatory

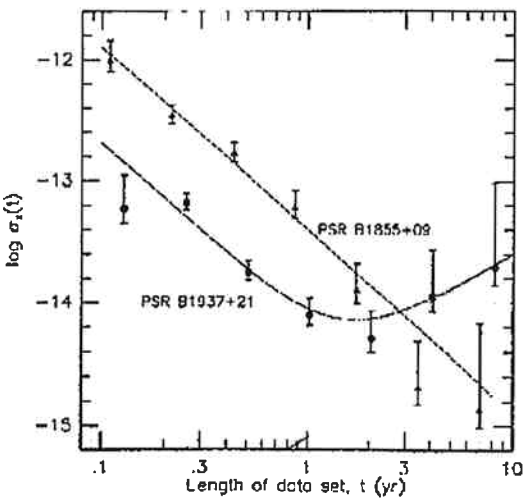

Fig. 1 Frequency stability of the millisecond pulsars PSR1937+21 and PSR1855+09[1] (results obtained with the Arecibo 305 m antenna).

in France (equivalent to a 93 m dish), Jodrell Bank in the UK (76 m), Green Bank in the USA (43 m), the Parkes observatory in Australia (64 m), Effelsberg observatory in Germany (100 m), and Kalyazin in Russia (64 m). However, these observatories are mainly involved in astronomical research, and there are currently only a few researchers whose work relates to frequency standards.

Research into pulsars at CRL began in 1989 once the 34 m antenna had been installed at the Kashima Space Research Center. Our research focuses on three main areas: theoretical research into timing accuracy and the like[7], VLBI observations of pulsars in collaboration with other countries such as Russia[8], and millisecond pulsar timing measurements. With regard to the timing measurements, we started by developing our own observation system. This involved developing technology for measuring the timing of extremely feeble pulses with high accuracy. Although the 34 m antenna is a much smaller antenna than the observatories mentioned above, we nevertheless managed to make successful observations in 1992 of the millisecond pulsar PSR1937+21 with an experimental observation system (based on a 270 kHz × 16 channel filter bank, and with a receiving bandwidth of 4 MHz). The measurement precision of these observations was about 18 μs, which demonstrates the feasibility of millisecond pulsar observations with a 34 m antenna[9]. After that, improvements were made to the system, and in 1997 a new system with an available bandwidth of 200 MHz was completed. Instead of using a filter bank as employed in many other stations, this pulsar observation system is unique in that it uses an acousto-optic spectrometer (AOS). By developing a special-purpose data processing system we also made the system capable of performing long-term integration in real time. As a result of such enhancements, the daily observation precision of PSR1937+21 was improved to 2.9 μs. This level of precision constitutes a significant achievement, considering that it was obtained with an antenna whose area is a hundred times smaller than that of the Arecibo 305 m antenna (which has an observation accuracy of 200 ns). From a technical viewpoint, the development of this highly precise timing measurement system involved bringing together and making advances in various technologies that have so far been cultivated by CRL, such as precise measurement techniques for frequency standards, time comparison techniques, and techniques for making astronomical observations with a 34 m antenna. CRL is playing an important role in this research. Since autumn 1997, we have used the system to make routine weekly observations, and we have been the only observatory in Japan making continued observations of a millisecond pulsar.

This report presents an overview of the observation system developed here, and describes the current status of our continuous observations.

2. Observation System

2.1 The characteristics of pulsar signals

Before describing the system, we will list the properties of pulsar signals that should be considered when making timing measurements.

(*A*) *The signals are weak (low flux density).*

Millisecond pulsars have exceedingly weak signals. For example, the most intense millisecond pulsar in the northern sky is PSR1937+21. But the flux density $\langle S \rangle$ of this pulsar (calculated in the 2.2 GHz band) is only about 3 mJy[11], where one Jansky (Jy) is equivalent to 10^{-26} $Wm^{-2}Hz^{-1}$. This is about a thousand times fainter than the quasars used as radio wave sources for VLBI.

(*B*) *The signal intensity is roughly inversely proportional to the square of frequency.*

For example, the intensity of PSR1937+21 is represented by the following equation[11].

$$S(f) = S(1\ \mathrm{GHz}) \times f^{\alpha}$$
$$S(1\ \mathrm{GHz}) = 25.9 \pm 2.6 \quad (\mathrm{mJy})$$
$$\alpha = -2.6 \pm 0.05 \qquad \cdots\cdots (1)$$

where f =observation frequency (GHz), $S(f)$ =flux density at f (mJy), and $S(1\ \mathrm{GHz})$ =flux density at 1 GHz (mJy). The signals are stronger in lower frequency bands, which makes observations easier, but in low frequency bands, problems are caused by smearing of the pulse waveform due to the effects of (C) below.

(*C*) *The signals are dispersed by interstellar plasma.*

This causes a frequency-related shift occurs in the pulse arrival times. During the propagation of a pulsar signal, it is delayed by interstellar plasma according to the following equation[12].

$$dt_{DM}(f) = 4.15 \times 10^{3} \times DM \times f^{-2} \quad (s) \cdots\cdots (2)$$

where f =observation frequency (MHz), and DM =Dispersion Measure (pc/cm^3) = total number of electrons per unit area in the line of sight. High frequency components arrive earlier, and low frequency components arrive later. In other words, when a pulsar signal is received over a wide bandwidth, its waveform is smeared due to the different amounts of delay. The spreading of pulse duration by dispersion can be calculated by transforming equation (2) as follows[12].

$$\Delta t = 8.3 \times 10^{3} \times DM \times f^{-3} \times B \quad (s) \cdots\cdots (3)$$

where B =bandwidth (MHz). For equal receiving bandwidths, the spreading of pulse duration increases for signals of lower frequency bands.

2.2 System design strategy

The aim of the observation system is to make precise measurements of the pulse timing of signals having the properties mentioned in section 2.1. Specifically, the pulse waveform is first detected from the background noise, and then the pulse's time of arrival is determined from the position of its peak. In the following equation, the measurement error σ_t of the pulse arrival time is derived as a function of the system sensitivity[13].

$$\sigma_t = \frac{W^{3/2} \cdot T_{sys}}{(B \cdot T \cdot P)^{1/2} \cdot \langle S \rangle \cdot G} \qquad \cdots\cdots (4)$$

where W =half width of observed pulse (s), P =pulse period (s), T_{sys} =system noise temperature (K), $\langle S \rangle$ =average flux density of pulse (Jy), B =receiving bandwidth

(Hz), G =antenna gain (K/Jy), and T =integration time (s).

The 34 m antenna has a much smaller aperture (lower G) than the Arecibo and Nancay telescopes, so for our system it was essential to increase the receiving bandwidth B and integration time T. It was also necessary to increase the time resolution so that pulse waveforms of the order of a few tens of microseconds wide could be reproduced.

2.3 Characteristics of the CRL observation system

The basic requirements of the system design are: (i) wideband receiving, (ii) long-period integration, and (iii) high time resolution. To fulfill requirements (i) and (iii), we had to introduce AOSs and fast CCD cameras, and for requirement (iii) we had to develop a dedicated processor. These components are described below.

To achieve a wide observation bandwidth, we set ourselves the target of receiving signals over the entire IF band. Since our observations were made in the 2 GHz band (2150-2350 MHz), we therefore aimed to make the system capable of processing signals received over a bandwidth of up to 200 MHz. Since dispersion delay (2.1(C)) causes serious smearing of the signals over such a wide bandwidth, we employed a method whereby the wideband signal is partitioned into separate channels, and then the delay of each channel is corrected. This allows the spreading of the received pulse duration to be more or less confined to the amount of delay occurring within the bandwidth of a single channel. To suppress the pulse corruption in the 2 GHz band to about 10 μs (the extent of time resolution), Equation (3) shows that it has to be partitioned into individual channels with a bandwidth of approximately 200 kHz. Although many observatories use filter banks to implement frequency division techniques, it would be unrealistic to use a bank of 200 MHz/200 kHz=1000 filters. Instead, we decided to use an AOS[14], which is an efficient frequency division tool.

An AOS is a frequency divider that utilizes next principle. When laser light and electrical signals are input into an acousto-optic element, the laser light is diffracted through an angle corresponding to the frequency of the input electrical signal. The intensity of the electrical signal can be inferred from the intensity of the diffracted light. The diffracted light is extracted in the form of an electrical signal by a CCD camera. Each CCD element thereby corresponds to a separate band channel. The introduction of an AOS made it possible to produce a compact system because a single acousto-optic element measuring just a few cm can partition a 50 MHz band into 256 channels.

The time resolution of an AOS is limited by the readout speed from the CCD camera. Since millisecond pulsar timing measurements require a time resolution of about 10 μs, we selected a CCD camera capable of high-speed data readout, and thereby obtained an AOS suitable for practical use as a timing measurement device for millisecond pulsars.

The 34 m antenna is better suited to long-period integration because it is able to track stars, unlike large-aperture fixed antennas that have to wait for stars to enter their field of view. In principle, it is also possible to integrate between successive pulsar observation sessions. In this case, the number of pulse additions for a millisecond pulsar can easily exceed ten million. To perform this huge addition processing efficiently, we developed a new dedicated processor. By using a design in which the data acquisition and calculation operations are performed concurrently, and in which dead time in the calculations is

Table 1 Various parameters of CRL's millisecond pulsar timing measurement system

Antenna		
	Aperture	34 mϕ
	Observation frequency	2.2 GHz
	System noise temperature	71 K
	Antenna gain	0.426 K/Jy
Signal processing unit (including AOS)		
	Band partitioning method	AOS
	Receiving bandwidth	200 MHz (50 MHz × 4 units)
	Frequency resolution	200 kHz 50 MHz / 256ch
	Sampling number	100 / period
	Time resolution	Approx. 16 μs
Averaging processor		
	A/D conversion	8 bit
	No.of pulse additions	Max. 2^{24}

suppressed as much as possible, we are able to obtain the integration results in real time while the observation is still in progress. Table 1 lists some of the important parameters of our observation system.

2.4 Data acquisition system

A block diagram of the system is shown in Fig. 2. We decided to make our observations at S-band frequencies so as to achieve a balance between intensity attenuation and the amount of distribution delay (see 2.1(B) and (C)). The system was also required to make observations in the L-band, but these were not easy due to the large amount of radio interference. Although the polarizer is capable of selecting either right-handed or left-handed circular polarization, we used right-handed circular polarization. The IF signal is first divided by a frequency converter into 50 MHz × 4 units, and four AOSs are then used to divide the signal from each unit into 256 channels. The frequency resolution is about 200 kHz. Since the AOSs use laser diodes and are therefore prone to frequency drift, their frequencies are periodically calibrated by using a carrier signal.

The AOS outputs are transferred serially to an averaging processor. This serial transfer is clocked by a signal synchronized to 1/100 of the pulsar period, which becomes the time resolution of the sampling. In the averaging processor, the processing for each individual AOS unit is assigned to a single board. The data for 256 channels which is sent in every 1/100 of pulsar period is subjected to 8 bit A/D conversion and stored in memory, and every period the data for the same phase in the same channel is added together. The boards are capable of performing these additions for up to 2^{24} (about 16 million) cycle periods.

2.5 Timing control system

The pulse addition timing must be perfectly synchronized to the pulsar period. However, the observed pulsar period changes continuously due to factors such as the Doppler effect caused by the Earth's motion, so a computer (Host #2) calculates a predicted period which is used to control a synthesizer in real time. This predicted period is calculated in real time by interpolating between values pre-calculated using the "TEMPO" program (see section 3) for each four-hour period. Signals synchronized to the predicted period P are supplied from the synthesizer to a clock-signal-generator. This clock-signal-generator produce serial transfer clock signals with a period of $P/100$, which are sent to the AOSs as data transfer triggers (sampling triggers), and clock signals synchronized to a period of P which are sent to the processors as averaging triggers.

A frequency standard with good short term stability is indispensable for pulsar timing observations. For example, if the averaging trigger stability is only around 10^{-9} (as achieved with ordinary quartz oscillators), then an error of about 10 μs will develop during integration over a three-hour period. The 34 m antenna, which is also part of a VLBI observatory, has a hydrogen maser, and all the oscillators can attain a short-term stability of about 10^{-13} by synchronizing their phase to the hydrogen maser reference signal.

The start time of an observation is obtained by reading the hours, minutes and seconds from a laboratory clock, while the fractions of a second are obtained from a time-interval-counter which measures the time difference from the 1 pps data acquisition start trigger of the laboratory clock. Since the laboratory clock measures time by counting up the 1 pps signals from the hydrogen maser, the time difference with UTC needs to be monitored by a GPS receiver. This time difference data is used for time correction during analysis.

2.6 Observation procedure

Host #1 is assigned to controlling the data acquisition. After various parameters (such as the number of additions) have been set up in the processor, it is put on stand-by until the time of observation. When the start time has been reached, a trigger to start data acquisition is output to the processor from the PIO board in the host #1. The data is stored in the hard disk of the host #1 after the addition has been completed. Four types of data are stored —(i) addition data (averager output; 100 samples × 256 ch per period, number of additions), (ii) a log file, which is recorded by an observation control program (pulsar name, observed frequency, etc.), (iii) the addition start time (time difference between start

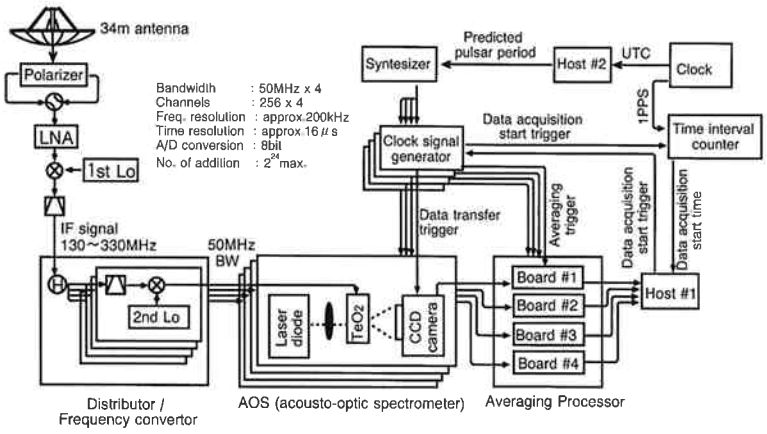

Fig. 2 The millisecond pulsar observation system using the 34 m antenna S-band system.

trigger and 1 pps signal as measured by the counter), and (iv) the time difference between the observation time and UTC (the laboratory time is constantly monitored by a GPS receiver). The database of the predicted period is also required in the analysis. After the observation has been completed, the distributed delay of each channel in each unit is compensated and synthesized off-line. Since the compensation quantities are rounded to 100 divisions per cycle —which is too coarse— the intervals between the sampling points are then further subdivided by a factor of 10 using a linear approximation. in this way, the delay can be compensated with a resolution of one thousandth of a cycle. The peak points are determined from the final waveform obtained in this way, and the pulse time of arrival is obtained from the phase and start time thereof. The above constitutes the primary process. In the analysis, the arrival time of each pulse as obtained in the primary process is compared with the predicted value obtained by calculation from a timing model, and the residual difference is obtained (see section 3).

3. Observation Results

3.1 Pulse waveforms of PSR1937+21

The above system was completed in 1997, and since November of the same year it has been making routine observations of the millisecond pulsar PSR1937+21. We chose this pulsar as our first target because it is the most intense in the northern sky and has been the subject of long-term observations at other observatories, which provide a useful source of data for checking the system. Observations were made on one day each week during the four hour period before and after the meridian transit of the pulsar. Each session involved performing addition for about 30 minutes, and observations were made every hour. From 5 to 8 sessions were performed per day. The observations were made at S-band frequencies (2120-2320 MHz), and in right-handed circular polarization.

Figure 3 shows the pulse waveforms observed on individual days. These results were obtained by combining the signals from 256 channels (50 MHz bandwidth) in one unit. This figure illustrates how the results can differ depending on the S/N ratio on the day in question. Although these observations were made under the same conditions, there are sometimes pronounced differences in the S/N from one day to the next.

3.2 Phase drift of pulse peaks

The peak phase determined from the observed waveform is converted into the time of arrival, and the residual is determined by comparing it with the predicted value. To calculate the predicted values, we used the "TEMPO" analysis program, which is produced by the pulsar group at Princeton University. TEMPO calculates the residuals after converting the pulse time of arrival at the observatory into the time of arrival at the solar system barycenter (SSB). The transformation equation is as follows[1][15].

$$t_b = t - D/f^2 + (\boldsymbol{r}\cdot\boldsymbol{n})/c + \Delta c + \Delta E - \Delta S \quad \cdots\cdots (5)$$

where t_b =time of arrival at SSB, t =time of arrival at observatory, f =observation frequency, D =dispersion constant, $\boldsymbol{r}$ = vector from SSB to the observatory, $\boldsymbol{n}$ = unit vector from SSB to the pulsar, Δc = time difference between the laboratory clock and reference time scale, ΔE =gravitational redshift due to planetary motion (Einstein delay), and ΔS = delay due to gravitational fields in the propagation path (Shapiro delay). Ephemerides are required for the model calculations, and DE200 was used in the present analysis. UTC was used as the reference time scale. The predicted pulse phase at SSB at time t_b is calculated next. The pulse timing at SSB can be regarded as being almost the same as the pulse timing produced by the pulsar itself, so the pulse phase at the solar system's center of gravity can be predicted in the following way from the pulsar's own rotation speed attenuation[1][15].

$$\phi(T) = \phi_0 + \nu T + \dot{\nu} T^2/2, \quad T = t_b - t_0 \quad \cdots\cdots (6)$$

where T = elapsed time from a certain epoch t_0 at the solar system's center of gravity, ϕ_0 = phase at the epoch (phase at $T=0$), and ν = rotation frequency. Since t_b is the time at which each pulse arrives at SSB, $\phi(T)$ should always be constant (or, by selecting a suitable value for t_0, zero). But in practice, when the value of t_b determined from the observed value of t includes errors and the model calculations of Equations (2) and (3) are not accurate, this can also lead to errors, so $\phi(T)$ does not become zero perfectly. These appear as residuals.

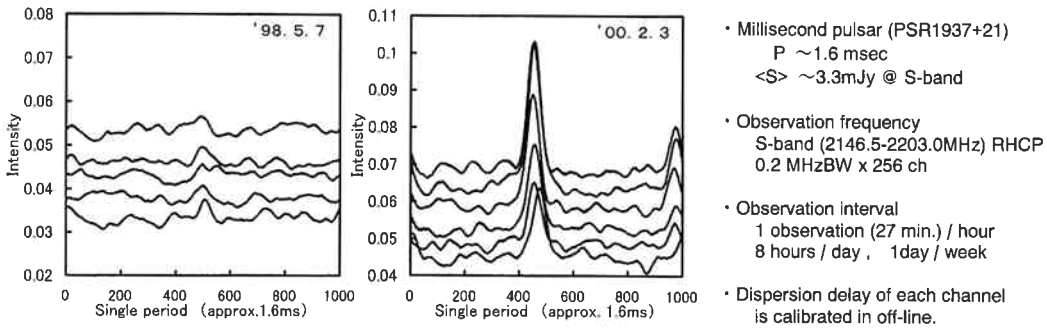

Fig. 3 Pulse waveforms of PSR1937+21. Waveform after integration for about 27 minutes in a single AOS unit (50 MHz bandwidth). This figure shows daily observation examples for a day with a good S/N and a day with a bad S/N.

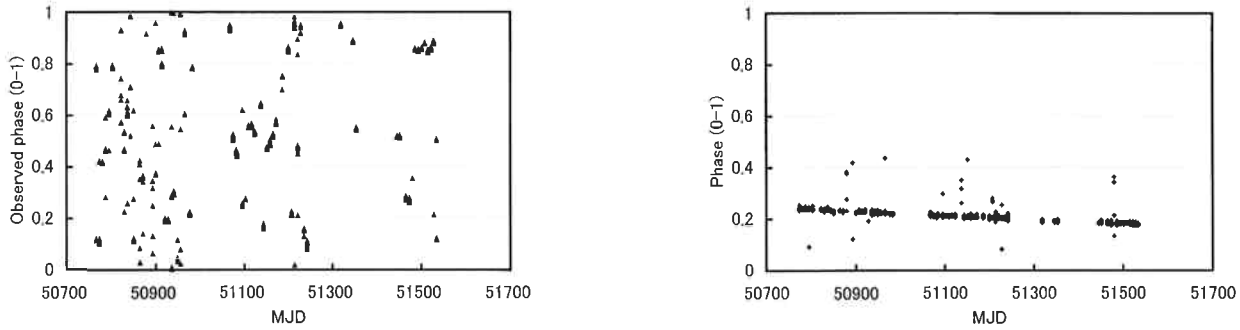

(A) (B)

Fig. 4 (A) Observed peak phase of PSR1937+21. The peak phases for each observation day are scattered because the observation start times are arbitrary. (B) Phase residual after predicted phase cancellation. The residuals roughly converge on a constant value. The predicted values more or less follow the observed phase.

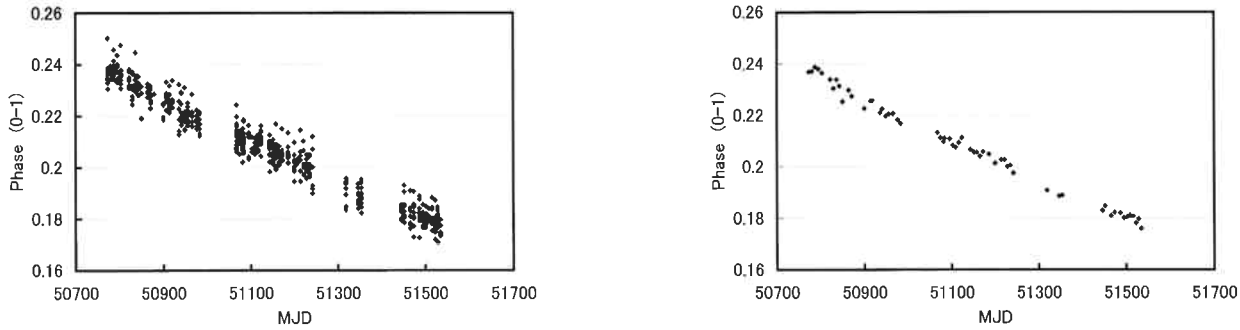

(A) (B)

Fig. 5 (A) An enlarged view of Fig. 4 (B), showing the fluctuation of peak phase in a 27 minute integrated waveform. After eliminating first-order trends, the standard deviation is 6.6 μs. (B) A plot of the average phase on each observation day. After eliminating first-order trends, the standard deviation is 2.9 μs.

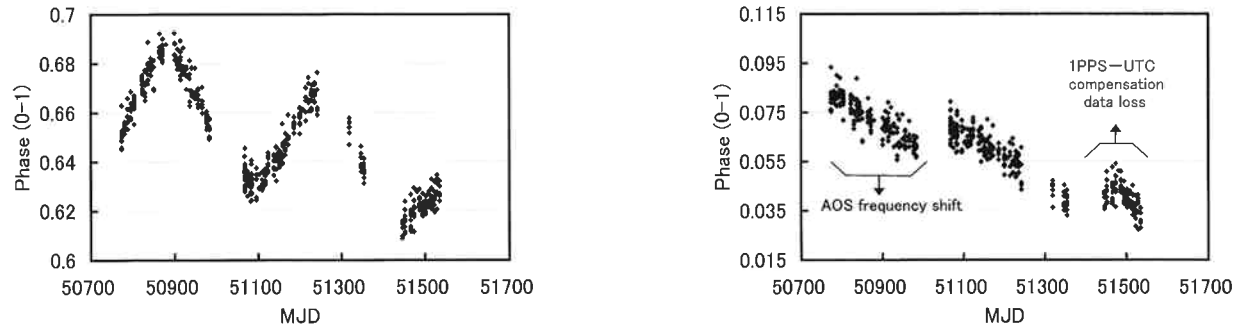

(A) (B)

Fig. 6 (A) Phase residual when analyzed using the DE405 ephemerides. A large annual drift occurs compared with the results of calculations using DE200 (Fig. 5). (B) Apparent phase drift resulting from inadequate observation time/frequency correction.

Figure 4 shows the phase drifts obtained from observations made between November 1997 and December 1999. Here we used the results obtained with one unit (50 MHz BW) and 27 minutes' integration. The data from the other three units was not synthesized due to problems such as defective periods. Figure 4 (A) shows the peak phase obtained from each observed waveform. Since the observation start times are arbitrary, the observed phases are scattered. The phases predicted from each of these values were canceled out (Fig. 4 (B)). It can be seen that the phase residuals become more or less constant, so the prediction calculation was more or less able to trace the observed phase

When data with large observation errors is eliminated and Fig. 4 is enlarged, the long-term trend becomes clear (Fig. 5 (A)). This shows that the prediction calculation is not yet completely accurate—after removing first-order trends, the standard deviation became 6.6 μs. Next, we tried plotting the average phase obtained on each observation day (Fig. 5 (B)). This is equivalent to the phase drift that occurs when the integration time is increased by a factor of 5-8. The standard deviation is 2.9 μs, which is about $\sqrt{5}$ times better than the results obtained by integration for 27 minutes. As originally expected, the effects of long-term integration are immediately apparent.

As an experiment, we tried to calculate the effect of changing the ephemerides referred to in the calculations. In Fig. 4 (B) and Figs. 5 (A) and (B), the pulsar position obtained using DE200 (the value supplied to TEMPO) was used as the initial value in the calculation, and DE200 was also used in the analysis. But when the ephemerides used in the analysis was changed from DE200 to DE405 without changing the initial values of the calculation, a considerable annual drift appeared in the predictions (Fig. 6 (A)). This result arises naturally due to the inappropriate combination of the initial values of the calculation and the ephemerides it refers to, and it can thus be seen that widely differing results can be obtained depending on the analysis conditions.

Figure 6 (B) shows an example of the results obtained when errors were left in the observation time compensation and the AOS frequency correction. Although at first glance there appears to be an annual drift due to the large phase drift in two places, this drift disappeared when the observation conditions were suitably corrected. It can thus be seen that careful treatment of the observation conditions and prediction calculation conditions is essential when analyzing phase drifts.

4. Conclusion

With the aim of application to a millisecond pulsar time scale, CRL is developing an original observation system which uses a 34 m antenna, and has been making routine observations of the millisecond pulsar PSR1937+21 since 1997. We have achieved a timing observation accuracy of about 6.6 μs from the data obtained with an integration time of about 27 minutes, and about 2.9 μs from the data obtained in a single observation day (equivalent to an integration time of 2.5 to 4 hours). Since 100 m class antennas are generally used for the observation of millisecond pulsars, whose signal strength is extremely feeble, it may be said that the 34 m antenna is the smallest class of millisecond pulsar observatory. But with a backend adapted to wide band receiving and a long-time integral that exploits the benefits of tracking, we have been able to make up for the antenna's handicaps, allowing millisecond pulsars to be observed even with this class of antenna. Compared with the 305 m Arecibo telescope, which has an observation accuracy of about 200 ns, the observation error of our system is about 10 times larger. However, considering the area of its antenna is about 100 times smaller, it can be said that our system exhibits adequate performance. Ours is the only antenna in Japan making continuation observations of a millisecond pulsar, so it has an important role to play.

Areas for future work include eliminating the residual trends by parameter fitting, and making a detailed determination of the pulsar parameters. We will work toward revising the pulsar parameters so that the phase residual obtained by the least squares method is minimized. If the observation results and the prediction computation model are correct, then it should be possible to obtain suitable convergence values for each parameter, while at the same time eliminating the long-term trends in the phase residuals.

When the ephemerides used in the analysis were replaced with DE405, a large change was observed in the phase drift. If the pulsar position can be re-determined so that this phase drift is eliminated, then the pulsar position can be found on the basis of DE405. From the results of Fig. 5 (A) and Fig. 6 (A), it is expected that the pulsar positions according to DE200 and DE405 will differ considerably. A comparative examination of these positions should allow the ephemerides to be verified. It would also be interesting to compare our results with the positions obtained by VLBI. This is a matter for future study. The 34 m antenna has also been used in VLBI observations, and has been making VLBI observations of pulsars for several years together with Russia and Canada. We would like to make the most possible use of this merit of being able to implement timing observations and VLBI observations with the same antenna.

Acknowledgments

We are deeply indebted to everyone at the Kashima Space Research Center for their helpful advice and cooperation in the development of this system and in making the observations. We would also like to thank Cosmo Research Corp. for their help in developing the averaging processor, and Mr. Tsuchida of Nogawa Tsushinki Seisakusho for his assistance in developing the AOS equipment.

References

[1] V. H. Kaspi, J. H. Taylor and M. F. Ryba, "High-precision timing of millisecond pulsars. III. Long-term monitoring of PSRs B1855+09 and B1937+21", Astrophys. J., 428, pp.713-728, 1994.

[2] B. Guinot and G. Petit, "Atomic Time and the Rotation of Pulsars", Astron. Astrophys., 248, pp.292-296, 1991.
[3] R. S. Foster and D. N. Matsakis, "Application of Millisecond Pulsar Timing to the Long-Term Stability of Clock Ensembles", Proceedings of the 27th Annual Precise Time and Time Interval (PTTI) Applications and Planning, pp.311, 1995.
[4] G. Petit and P. Tavella, "Pulsars and Time Scales", Astron. Astrophys., 308, pp.290-298, 1996.
[5] N. Bartel, J. F. Chandler, M. I. Ratner, I. I. Shapiro, R. Pan, and R. J. Cappalo, "Toward a Frame Time Via Millisecond Pulsar VLBI", Astron. J., 112, No.4, pp.1690-1696, 1996.
[6] M. Hosokawa, "8.1 Overview of Pulsar Time Scale", Review of the CRL, 45, 1/2, pp.117-125, March/June, 1999.
[7] M. Hosokawa, K. Ohnishi, and T. Fukushima, "Uncertainty of pulsar time scale due to the gravitational time delay of intervening stars and MACHOs", Astron. Astrophys., 351, pp.393-397, 1999.
[8] M. Sekido, M. Imae, Y. Hanado, Y. P. Ilyasov, V. Oreshiko, A. E. Rodin, S. Hama, J. Nakajima, E. Kawai, Y. Koyama, T. Kondo, N. Kurihara, and M. Hosokawa, "Astrometric VLBI observations of PSR 0329+54", Publ. Astron. Soc. Japan, 51, pp.595-601, 1999.
[9] Y. Hanado, H. Kiuchi, A. Kaneko, and M. Imae, "Millisecond pulsar observation at CRL", J. Commun. Res. Lab., 40, No.2, pp.55-62, July 1993.
[10] Y. Hanado, M. Imae, M. Sekido, and M. Hosokawa, "8.2: Development of the observation system for pulsar time scale", Review of the CRL, 45, 1/2, pp.127-135, March/June, 1999.
[11] R. S. Foster, L. Fairhead, and D. C. Backer, "A spectral study of four millisecond pulsars", Astrophys. J.,3 78, pp.687-695, 1991.
[12] A. G. Lyne and F. Graham-Smith, "Pulsar astronomy", pp.28, Cambridge University Press, 1990.
[13] R. S. Foster and D. C. Backer, "Constructing a pulsar timing array", Astrophys. J., 361, pp.300-308, 1990.
[14] K. Akabane, N. Kaifu, and H. Tawara, "Cosmic radio wave astronomy", pp.337-340, Kyoritsu Shuppan, 1988.
[15] J. H. Taylor and J. M. Weisberg, "Further experimental tests of relativistic gravity using the binary pulsar 1913+16", Astrophys. J, 345, pp.434-450, 1989.